

# Hazards of Hypervelocity Impacts on Spacecraft

Shu T. Lai\* and Edmond Murad†

*U.S. Air Force Research Laboratory, Hanscom Air Force Base, Massachusetts 01731-3010*  
and

William J. McNeil‡

*Radex, Inc., Bedford, Massachusetts 01730*

Hypervelocity impacts by space particles, such as meteoroids and debris, pose hazards to spacecraft. The limits of velocity of meteoroid and debris are derived. Characteristic properties of hypervelocity impacts are momentum transfer, penetration, plasma production, localization, and suddenness. Using McDonnell's empirical formulas derived from laboratory experiments, impact penetrations and plasma production rates in the space environment are calculated. When the critical temperature theorem for Maxwellian space plasmas is used, the energy of the plasma generated is shown to be too low to induce any significant spacecraft charging. The plasma generated, however, can induce a transient, sustained or avalanche discharge between differentially charged surfaces. The discharge current depends not only on the plasma density generated but also on the neutral gas released on impact. A scenario of impact induced hazard following days of passage of a high-energy plasma cloud, such as a coronal mass ejection cloud, is discussed. Some mitigation methods are discussed. Finally, we discuss whether electrons can be accelerated to high energies in a meteor trail.

## Nomenclature

$A$	=	area, $\text{m}^2$
$d$	=	projectile diameter, m
$F$	=	normal component of meteor flux, $\text{m}^2 \cdot \text{s}^{-1}$
$f(E)$	=	electron distribution as a function of electron energy $E$
$I$	=	moment of inertia, $\text{g} \cdot \text{m}^2$
$M$	=	brightness in the astronomical scale (logarithm of the luminosity flux from a source)
$M_s$	=	spacecraft mass, g
$m$	=	meteor mass, g
$m_e$	=	electron mass, g
$P$	=	probability of meteor impact
$P_N$	=	probability of $N$ impacts
$p$	=	penetration depth, m
$Q$	=	charge production rate
$R$	=	spacecraft radius, m
$T$	=	electron temperature, keV
$T^*$	=	critical or threshold temperature for the onset of spacecraft charging, keV
$t$	=	time, s
$V$	=	projectile velocity, $\text{km} \cdot \text{s}^{-1}$
$V_f$	=	relative velocity, km/s
$V_o$	=	orbital velocity, km/s
$V_s$	=	escape velocity, km/s
$v$	=	meteor velocity, km/s
$Y_e$	=	yield of electrons emitted by a hypervelocity particle impact
$Y_i$	=	yield of ions emitted by a hypervelocity particle impact
$\alpha$	=	number of ionizations generated by an electron traveling through a distance $dx$
$\gamma$	=	number of electrons generated by an ion impact on a cathode

$\delta(E)$	=	coefficient of secondary-electron emission with primary electron energy $E$
$\eta(E)$	=	coefficient of backscattered-electron emission with primary electron energy $E$
$\mu$	=	number of ionizations generated by an electron traveling from the cathode to the anode
$\rho_p$	=	projectile density, $\text{g} \cdot \text{cm}^{-3}$
$\rho_T$	=	target density, $\text{g} \cdot \text{cm}^{-3}$
$\sigma(E)$	=	electron impact ionization cross section, $\text{cm}^{-2}$
$\sigma_{Al}$	=	tensile strength of aluminum
$\sigma_T$	=	tensile strength of target
$\omega$	=	angular velocity, rad/s

## Introduction

FOR any satellite, solar radiation and emissions, space plasma, energetic particles, and meteoroids provide sources of concern. Solar effects,<sup>1</sup> space plasma,<sup>2</sup> and energetic charged particle interactions<sup>3</sup> have been addressed in many papers over a period of years. Hypervelocity impacts by meteoroids and space debris on satellites have also been studied but mostly for astronomical applications.<sup>4</sup>

The latter topic, that is, hypervelocity impact, is the subject of this paper. Meteor impact may be separated into two distinct parts: 1) the probability of collision between a meteoroid and a satellite and 2) the effects arising from a collision between a meteoroid and a satellite. The probability that a meteoroid will collide with a satellite is proportional to the geometric cross section of the satellite and to the flux of meteoroids and other cosmic dust particles. A number of authors have calculated such probabilities<sup>5–8</sup> by taking into account meteoroid and dust fluxes.<sup>9</sup> Three types of interactions will be considered in the direct collisions with satellite surfaces: 1) penetration of the satellite surfaces, 2) collision with the surfaces, with consequent generation of a cloud of neutral atoms and dust, and 3) the formation of plasma on collision of the meteoroid with the satellite surface with the potential consequence of a sudden discharge.

The long-duration exposure facility (LDEF) had a six-year space sojourn, resulting in a treasure trove of debris- and meteoroid-impact data. Studies of craters on a variety of surfaces made possible a determination of the flux of particles as well as a qualitative discrimination between space debris and interplanetary dust or meteoroids.<sup>10,11</sup>

The penetration depth of hypervelocity impacts is found to have an empirical relationship that depends on the relative densities of the meteoroids and target, the meteoroid diameter, and the impact

Received 2 February 2001; revision received 15 July 2001; accepted for publication 20 July 2001. This material is declared a work of the U.S. Government and is not subject to copyright protection in the United States. Copies of this paper may be made for personal or internal use, on condition that the copier pay the \$10.00 per-copy fee to the Copyright Clearance Center, Inc., 222 Rosewood Drive, Danvers, MA 01923; include the code 0022-4650/02 \$10.00 in correspondence with the CCC.

\*Senior Research Physicist, Space Weather Center of Excellence, Space Vehicles Directorate, 29 Randolph Road. Senior Member AIAA.

†Technical Advisor, Space Weather Center of Excellence, Space Vehicles Directorate, 29 Randolph Road. Senior Member AIAA.

‡Senior Analyst.

**Table 1** Spacecraft failed and damaged due to meteoroid or debris impact<sup>a</sup>

Vehicle	Date	Effect	Possible cause
HST	April 1990	5000 impacts in 4 years, solar cell punctured.	Meteoroid/debris
ISEE-1	Oct. 1977	Detector window punctured.	Meteoroid
ISEE-1	Aug. 1978	All isobutane gas lost in 5 days.	Meteoroid
Olympus	Aug. 1993	Satellite failed to function.	Meteoroid
SEDS 2	March 1994	Mission terminated.	Meteoroid/debris
MSTI 2	March 1994	Satellite communication lost.	Meteoroid/debris
Kosmos-1275	July 1981	Fragmented into 200 pieces.	Debris
Solar-A	Aug. 1991	Telescope punctured.	Meteoroid
STS-45	March 1992	Gouges on wing edge.	Debris
STS-49	May 1992	Chip in window pane.	Debris

<sup>a</sup>Data adapted from Koons et al.<sup>18</sup> HST, Hubble Space Telescope; ISEE, International Sun–Earth Explorer; and STS, Space Transportation System.

velocity.<sup>12,13</sup> Laboratory simulations of the hypervelocity impact of debris on surfaces have been performed extensively. For example, in the impact of a 70-nm boron carbide particle ( $4 \times 10^{-16}$  g) at a speed of  $94 \text{ km} \cdot \text{s}^{-1}$  on an aluminum target doped with silver, the total energy of the products (vaporization, ionization and kinetic energy of products) represented about 3.7% of the projectile energy.<sup>14</sup> In addition to meteoroids, space debris represent another type of interaction that somewhat resembles the behavior of meteoroids. Because space debris is for the most part banded at an altitude near 1000 km, this interaction can be considered to be important in the altitude region 600–1600 km (Ref. 15). This hazard arises from the breakup of satellite and spent upper stages, leading to the presence of large amounts of debris.<sup>16</sup> It is estimated that the number of space debris objects greater than 0.01 m diam will increase from near 8000 in 2000 to ~180,000 in 2100 at geosynchronous orbit.<sup>17</sup> In view of the rapidly increasing number of spacecraft and the large increase in the number of space debris objects in the next century, hypervelocity impact on spacecraft systems needs to be considered as an important component of spacecraft interactions and spacecraft survivability.

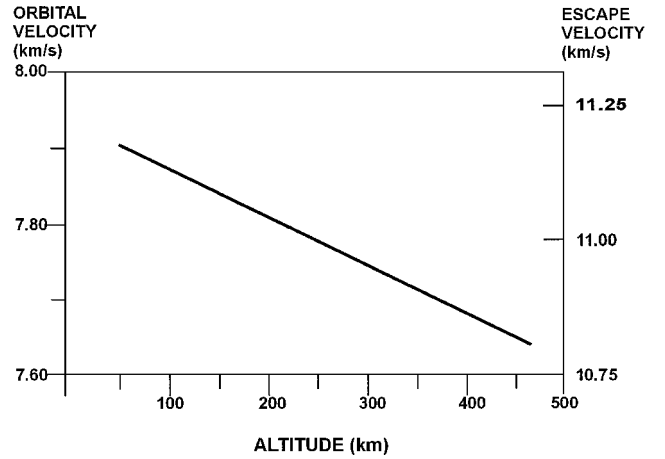
### Hypervelocity Impacts as Space Hazards

When meteoroids enter the atmosphere, they do so at velocities ranging from about 11 to  $72 \text{ km} \cdot \text{s}^{-1}$ . Space debris have orbital velocities of  $7\text{--}11 \text{ km} \cdot \text{s}^{-1}$  typically. These large velocities imply large kinetic energies and momenta.

For known events, we refer to the Koons et al.<sup>18</sup> list of missions lost or terminated due to the space environment from 1973 to 1997. Of the 10 cases listed in Table 1, four were due to meteoroid impacts, whereas the rest were attributed to debris or meteoroids/debris. The three spacecraft lost due to meteoroid impact are Olympus (August 1993), the Small Expendable Deployer System (SEDS) (2 March 1994), and the Miniature Sensor Technology Integration (MSTI) (2 March 1994).<sup>18</sup> Some of the electrostatic discharge cases could be due to meteor impact as well. Therefore, meteor and debris impacts on spacecraft constitute a considerable percentage of the total cases of space missions lost.

Whereas spacecraft interactions with space plasmas have been well studied,<sup>2,19</sup> our understanding of hypervelocity impacts on spacecraft are in a less mature stage of development. In this paper, meteoroid velocities, impact penetration depth, impact plasma production, and hazards of hypervelocity impacts are studied.

The organization of this paper is as follows. The velocities of meteors and the kinetic energies of atoms at such velocities are bracketed. Because of the tremendous impact kinetic energies, significant surface penetration may occur. Impact penetration depths are calculated using empirical formulas based on experiment. Two likely effects due to hypervelocity impact, namely, mechanical and electrical, are studied. Mechanical effects include surface or structural damage by impact penetration and perturbation of spacecraft linear and angular momenta. Electrical effects are due to plasma generation on impact. A most common concern is whether the impact-generated plasma can cause spacecraft charging and discharging. After examining the laboratory results for the energy of the impact-generated plasma, we conclude that meteoric impact is unlikely to cause significant spacecraft charging. The plasma, however, disturbs scien-

**Fig. 1** Orbital and escape velocities at various altitudes.

tific measurements. More significantly, the plasma can cause current leakage or even avalanche discharges between differentially charged configurations. Some most likely differentially charged configurations are solar cells, surfaces of very different properties, and double-layer deep dielectric charging.<sup>20</sup> These unstable configurations pose significant potential hazard for spacecraft. Another hazard involving both mechanical and electrical aspects is pointed out. If an impact penetrates through a wall, the impact-produced plasma can exit from both sides of the puncture. The plasma inside the wall may cause significant short circuits among the electronic components inside, this being a significant hazardous scenario. Finally, some mitigation techniques are discussed.

### Meteoroid and Debris Velocities

The escape velocity  $V_s$  of a particle from a point in the solar system and the orbital velocity  $V_o$  at the point are related by

$$V_s^2 = 2V_o^2 \quad (1)$$

A meteoroid at the Earth's location has an escape velocity  $V_s = 42.0 \text{ km/s}$ . For its head-on collision with the Earth, which has orbital velocity of  $29.7 \text{ km/s}$ , the relative velocity is  $42.0 + 29.7 = 71.7 \text{ km/s}$ . Including the Earth's gravitation, the maximum relative velocity  $V_f$  is  $72.6 \text{ km/s}$ .

The velocity needed to escape from Earth from an altitude of 120 km is about  $11.1 \text{ km/s}$ . Because the orbital velocity is related to the escape velocity [Eq. (1)] the orbital velocity of debris at 120 km is  $11.1/\sqrt{2} = 7.8 \text{ km/s}$  approximately (Fig. 1). Below that altitude, atmospheric drag becomes significant in the deceleration of meteorites and particulates.

If the eccentricity of the Earth's orbit is included, the Earth's orbital velocity ranges from  $29.3$  to  $30.3 \text{ km/s}$ , with heliocentric escape velocities of  $41.4\text{--}42.8 \text{ km/s}$ . As a result, the impact speeds could range up to  $73.1 \text{ km/s}$  or, when the gravitational attraction is taken into account, up to  $74.0 \text{ km/s}$ .

The preceding treatment assumes that all meteoroids are on closed solar system orbits. There is now conclusive evidence for a significant population of meteoroids that arrive from interstellar space. At

SPACE ENVIRONMENT	EFFECTS
Debris & Meteorites	Impact Penetration, Puncture, Plasma Production
Cosmic Rays	Single Event Upsets
Solar Eruptions	Shocks, Geomagnetic Storms
Radiation Belt Particles	Radiation Damage, Degradation, Deep Dielectric Charging
Energetic Plasma	Surface Charging & Discharging, Spacecraft Anomalies
Low-energy Plasma	Leakage, Erosion
Neutral O Atoms	Chemical Reactions, Erosion

Fig. 2 Energy scale of various spacecraft–environment interactions.

the mass range  $10^{-7}$  kg, they probably account for a few percent of the total meteoroid input. There are some radar records<sup>21</sup> indicating a tail of higher velocity meteors. Relatively recent reviews of the topic of detection of meteoroids with origin outside the solar system are given by Hawkes et al.<sup>22</sup> and by Ceplecha et al.<sup>23</sup>

### Impact Energy

Because of the large-impact-energy, hypervelocity impacts of meteoroids pose hazards to space systems<sup>24</sup> and human space flights.<sup>25</sup> A Leonid meteoroid of 0.1 g in mass, traveling at 71 km/s, would impact the solar cell of a spacecraft with a force equal to that of a bullet. A calcium atom, for example, traveling at 72 km/s has a kinetic energy of about 1 keV. Therefore, a meteoric particle, often with more than millions of atoms, has a kinetic energy exceeding 1 GeV. Both debris and meteoric particles can cause physical damage. Debris and meteoric impacts are the most energetic interactions compared with all others, such as impacts by neutral oxygen atoms in the ionosphere, hot plasmas at geosynchronous orbits, energetic electrons and ions in the radiation belts, coronal mass ejection particles, and cosmic rays (Fig. 2).

Fast atoms and ions can penetrate into surfaces on impact generating ionization tracks inside the solid, ejecting plasma and neutral gas vapor to outside the surface, and, if puncture occurs, spraying plasma and energetic projectiles to behind the solid wall. Some of the hazardous effects are discussed in a later section.

### Impact Penetration

Cour-Palais<sup>26</sup> measured in the laboratory the penetration depth  $p$  as a function of the impacting particle diameter  $d$ , density  $\rho$ , and velocity  $V$  and obtained an empirical equation,

$$p/d^{1.056} = C \rho_m^{0.519} V^{0.7} \quad (2)$$

where  $\rho_m$  is in grams per cubic centimeter,  $V$  is in kilometers per second, and  $C$  is a constant that is characteristic of the target material and its condition. An approximate formula based on LDEF observations is given in Tribble<sup>27</sup>:

$$p = K m^{0.352} \rho_T^{1.667} V^{0.875} \quad (3)$$

where  $m$  is the mass (grams) of the particle,  $\rho_T$  the target density (grams per cubic centimeter),  $V$  the normal component of the particle velocity relative to the surface, and  $K$  a materials constant.

McDonnell and Sullivan<sup>11</sup> and McDonnell et al.<sup>13</sup> obtained an empirical equation for meteoroids and debris impacts applicable under a wide range of target densities  $\rho_T$  and tensile strengths  $\sigma_T$ :

$$p/d = 0.7658 d^{0.056} (\rho_p/\rho_T)^{0.476} (\sigma_{Al}/\sigma_T)^{0.134} V^{0.806} \quad (4)$$

Note that these formulas are approximate because they are based on laboratory experiments with solid particles. In space, the meteoroids are likely to be fluffy and irregularly shaped<sup>28</sup>; hence, the actual

densities and tensile strengths may be incorrectly represented in the preceding formulas.

Using the McDonnell et al.<sup>13</sup> formula [Eq. (4)], we have calculated the penetration depth to be 0.35 mm for a  $1.3 \times 10^{-5}$  g Leonid meteoroid colliding with a typical satellite mylar surface at 71 km/s. A penetration of 0.35 mm into typical solar panel Mylar<sup>®</sup> surface would cause damage on spacecraft solar panels. The effect of such a penetration may put out a single solar cell, leading to degradation of performance over time. A  $2.9 \times 10^{-4}$  g Leonid meteoroid would penetrate 0.01 m into aluminum. It is difficult to predict how damaging an impact penetration would be because it would depend on the details of what systems were near the impact. Penetrations followed by plasma and current generations, to be discussed later, would be more hazardous, affecting wider areas.

A comparison of formulas (3) and (4) is now discussed. The penetration depth  $p$  obtained by using the LDEF formula [Eq. (3)] is 0.09 m for the  $2.9(-7)$  kg particle. This is compared to 0.01 m using McDonnell's formula [Eq. (4)]. The problem with using LDEF data is that they do not include any impacts from particles this large. Note the small probability of such an impact even in a very large Leonid storm. LDEF really stops at about  $1(-8)$  kg as far as anything that is statistically meaningful.

### Impact Probability

The probability  $P$  of impact by a particle on a surface is given by

$$P = \int_t^{t+\Delta t} dt F(t) A \quad (5)$$

where  $\Delta t$  is the duration of the exposure and  $F(t)$  the normal component of the flux of particles. To calculate the probability of a given impact penetration depth  $p$ , one uses McDonnell's formula [Eq. (4)] to get a minimum diameter  $d$  to cause the event. With an assumed particle density, this gives the mass  $m$ . An empirical relationship between mass  $m$  and brightness  $M$  on the astronomical scale, which is a logarithmic scale of luminous flux from a source, is given by<sup>29</sup>

$$\log_{10} m = -0.4M - 10.97 + 1.7 \log_{10} V \quad (6)$$

where  $V$  is in centimeters per second. Then the meteor shower distribution function, a function of brightness  $M$  or mass  $m$ , gives one the flux  $F(t)$ . That, along with the area  $A$ , gives the probability [Eq. (5)].

The slope of the meteor shower distribution function is commonly characterized by the so-called population index  $r$ , which gives the relative number of meteors detected in successive divisions of unit magnitude  $M$ . Equation (6) is applied to meteor mass at the limiting magnitude  $6.5M$ . Details on modeling Leonids meteor shower population distribution as a function of meteor mass is given in Ref. 30.

Whereas Eq. (6) has been used for over 40 years, more recent observational work<sup>31,32</sup> seems to suggest slightly different values of the numerical factors. Recent studies<sup>33–36</sup> have suggested different mass–magnitude relationships. For our purposes, however, Eq. (6) seems adequate.

The meteoroid flux is expected to be unchanged from the entry point down to about 120 km, where meteoric ablation due to frictional heating begins. We examine two cases, the penetration of an unshielded solar cell and the penetration of a heavily shielded spacecraft surface. For the first case, we model the penetration as a 5-mm pit in a Mylar surface. The smallest Leonid needed to form this pit is 0.35 mm in diam and weighs  $1.3 \times 10^{-5}$  g. For a major Leonid storm such as that of 1966, the flux of such particles is  $8.63 \times 10^{-8} \text{ m}^{-2} \text{ s}^{-1}$  and, assuming  $20 \text{ m}^2$  of surface area and a 2.5-h storm, the probability of such a hit is 1.3% according to Eq. (5). In the second case, we assume a 0.05-m pit in an aluminum surface, which requires a Leonid meteor of 4.4-mm diam or 0.028 g. Again for a major Leonid storm, the flux would be  $4.69 \times 10^{-10} \text{ m}^{-2} \text{ s}^{-1}$  and the probability is 0.008%.

From elementary probability theory, the probability  $P_N$  of  $N$  impacts, each one of which is uninfluenced by the other, in a duration  $\Delta t$  is given by the Poisson distribution:

$$P_N = P^N \exp(-P)/N! \quad (7)$$

If  $N = 1$  and  $P \ll 1$ , one recovers Eq. (5) from Eq. (7) by using the Taylor expansion of the exponential.

### Impact Probabilities of Annual Meteor Showers

In the last section, some probabilities were quoted for penetration of a solar panel surface and a heavily shielded 0.05-m aluminum panel during a Leonid storm of historic magnitude. Here, these probabilities are compared to those encountered routinely by spacecraft during the annual meteor showers.<sup>22</sup> Three impact penetration scenarios are defined, and for each material, a critical penetration depth and a surface area exposed to the meteor stream need to be defined. First, a 5-mm penetration into a Mylar surface, which would most likely shatter a solar panel segment, is chosen. Using the DSCS satellite as typical, the exposed surface area of solar panels is around 20 m<sup>2</sup>. The second case is for a lightly shielded surface of the spacecraft. This could be, for example, an antenna section or a surface containing scientific instruments. Here a critical penetration of 10 mm in aluminum and a surface area of 10 m<sup>2</sup> are assumed. Only one face of the satellite would be exposed to the flux at any given time. For the third case, the equivalent of the critical spacecraft design shield (CSDS),<sup>8</sup> which is defined by a 49-mm pit in aluminum, is selected. The exposed area is taken to be 10 m<sup>2</sup> as typical of a medium-sized spacecraft.

We show in Fig. 3 the impact rates of the annual meteor showers for an equivalent penetration of one CSDS unit in aluminum, throughout the year, and, similarly, in Fig. 4, the impact rates for a 1-mm penetration in aluminum. In terms of maximum rate, the storm Leonids (LEO in Fig. 4) are the most likely, but the duration of the Leonids is relatively short compared to, for example, the  $\eta$ -Aquadrids (ETA in Fig. 4). It is the combination of peak intensity and duration that ultimately determines the probability of an impact

**Table 2** Some major showers and impact probabilities

Shower	Characteristics			Impact probability, %		
	Dates	ZHR	V	Case 1	Case 2	Case 3
Leonid storm	17 Nov.	150,000	71	2.00	0.067	0.0036
Annual leonids	14 Nov.–21 Nov.	23	71	0.48	0.0086	0.00003
$\eta$ -Aquadrids	19 April–28 May	37	66	2.32	0.035	0.0002
Perseids	17 July–24 Aug.	84	61	4.39	0.058	0.0003
Orinids	2 Oct.–7 Nov.	25	67	2.48	0.029	0.0001

from a particular shower. We see that the probability for impact is distributed pretty much uniformly throughout the year, with a relative lull in January–March (solar longitude  $>270^\circ$ ). Parameters for the showers are taken from Ref. 37.

In Table 2 we have compared probabilities for the three model impact scenarios for a major Leonid storm and for four of the most intense annual meteor showers. The mass distributions used to compute the flux of the limiting mass required to inflict the penetration were computed as described by McNeil et al.<sup>30</sup> The ranges of dates chosen for the calculation are those listed for these showers by the International Meteor Organization's Meteor Shower Calendar (available on line at URL: [www.imo.net](http://www.imo.net)). Note that, in computing the probabilities in Table 2, a relatively complete list of 50 major annual showers, compiled by Jenniskens,<sup>37</sup> was used, and therefore, the total probabilities contain contributions from other less intense showers during these time periods. Even so, this represents the total flux that a satellite would encounter during the time periods listed.

Note that, for cases 1 and 2, penetration of 0.005 m of Mylar and 10 mm of aluminum, the probabilities from the annual showers are comparable to and often greater than those from a truly historic meteor storm like the Leonids in 1966. This result arises from two factors. First, the storm is of short duration, a matter of hours, while some annual showers last from a few weeks to a month, albeit not at their maximum zenith hourly rate (ZHR). Second, the mass distributions of the annual showers favor smaller particles, whereas the storm, with its relatively fresh cometary ejecta,<sup>38</sup> has a disproportionately large number of larger meteors. It is only for the truly catastrophic impacts, such as case 3, where the Leonid storm poses more of a hazard, and even then, only with a very small probability and only a factor of 10 greater than the annual showers.

The probabilities for penetrating a solar panel, case 1, are relatively large and, over the course of a year, add up to one chance in five or so. Over a year, the probability of penetration of a lightly shielded surface on a single satellite is about 1 in 1000. This may seem small, but assuming 1000 satellites in orbit, such a penetration on at least one of them becomes likely. The probability of penetration of a heavily shielded surface, even during a Leonid storm, remains small. However, note that this increases linearly with exposed area. For a very large object, such as a space station, with 1000-m<sup>2</sup> exposed area, the probability of a 0.01-m penetration rises to 6% during a Leonid storm, with the probability for a CSDS penetration at 0.36%. These are not negligible, especially on crewed spacecraft. Finally, note that, in general, satellites are not designed with the CSDS level of protection, so that damage may certainly take place with impacts from particles significantly smaller than those implied by this limit.

### Perturbation of Angular Momentum

To estimate the effect on angular momentum, a spherical spacecraft of mass  $M_s = 10^5$  g, radius  $R = 2$  m, and a solar panel extending 10 m is considered. A Leonid meteor of velocity  $v = 72$  km/s and mass  $m = 0.1$  g, colliding with the tip of a boom or an extended solar panel would add an angular velocity  $\Delta\omega$  given by

$$I \Delta\omega = mvr \quad (8)$$

where  $I$  is the moment of inertia of the spacecraft,  $m = 0.1$  g,  $v = 72$  km/s, and  $r = 12$  m. For a sphere, the moment of inertia is given by  $I = (\frac{2}{5})M_s R^2$ . The result is  $\Delta\omega = 0.54 \text{ rad} \cdot \text{s}^{-1}$  or 0.086 Hz. This magnitude of spin rate change, by itself, is not significant and would not disrupt spacecraft operations. Nevertheless, it is detectable in certain telemetry signals such as electric field measurements by means of booms rotating with the spacecraft. One way

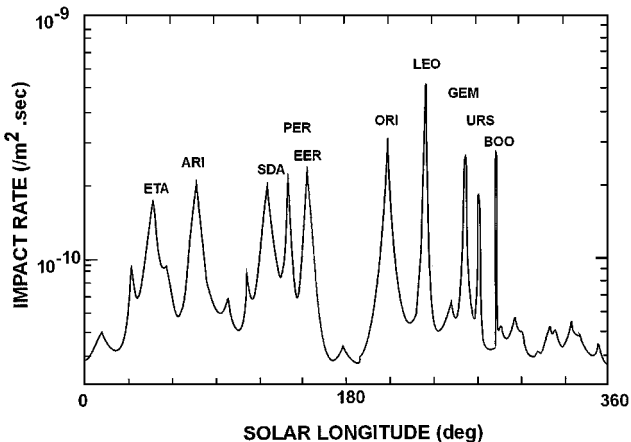


**Fig. 3** Annual distribution of the probability per square meter per second of meteoroid impact to 1 CSDS unit (4.9 mm) in aluminum.

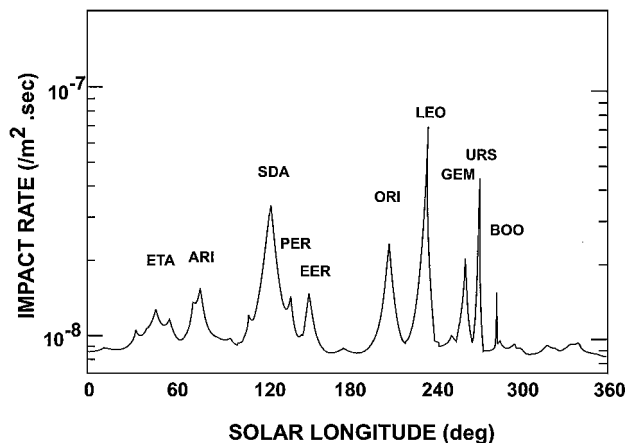


**Fig. 4** Annual distribution of the probability per square meter per second of meteoroid impact to 1 mm in aluminum.

to differentiate a meteor impact from one by a debris is to look at the vector direction of the sudden change of spacecraft angular momentum, from which one deduces the direction of impact. Typically, debris have near circular orbits, depending on the satellite from which the debris comes, and are much heavier but slower (at  $15 \text{ km} \cdot \text{s}^{-1}$  for head-on collisions at low Earth orbits) than meteoroids.

### Total Charge Production

When a meteor collides with a surface, the collision energy is enough to generate a plasma cloud on the surface. McDonnell et al.<sup>13</sup> obtained from extensive laboratory experiments an empirical formula for the electron charge production rate  $Q$ , when a meteoroid collides with an aluminum surface:

$$Q = 10^{-0.88} m^{1.02} (V/5)^{3.48} \quad (9)$$

The charge production rate is calculated for minor, moderate, and major Leonid showers of ZHR = 100, 5000, and 150,000, respectively. Assuming a population index of 1.8 for the Leonids<sup>39</sup> one obtains the time-averaged charge production rates during a 3-h storm period as  $0.2 \times 10^{-4}$ ,  $1.0 \times 10^{-3}$ , and  $3.0 \times 10^{-2} \text{ nA/cm}^2$ . For comparison, the average quiet time ambient flux of charged particles on SCATHA at near geosynchronous altitudes was calculated by Purvis et al.<sup>40</sup> to be  $0.115 \text{ nA/cm}^2$ . Similar results of quiet time geosynchronous altitude ambient flux have been obtained by using the current-voltage cutoff point of electron beam emission from SCATHA.<sup>41</sup> Thus, the time-averaged meteor impact generated charge flux is less than the ambient flux at quiet times on SCATHA. According to this analysis, the time-averaged meteor flux would not induce significant charging. However, meteor impacts are different from average flux both because they are localized and nearly instantaneous. It is difficult to say whether these differences would cause unwanted effects. There are other independent reasons why charging by meteor impact is unlikely, however, which we discuss in the next section.

### Can Meteor Impact Induce Spacecraft Charging?

It is common to associate the rate of plasma production by meteor impact with the likelihood of spacecraft charging, although that association has never been established. If meteor impact can induce hundreds or thousands of volts on spacecraft, it would be significant. We show next that this is very unlikely.

Before we discuss theory, we show an interesting observation (Fig. 5) that tempts one to associate instantaneous spacecraft charging with meteor impact. In Fig. 5, the lower panel plots the  $k_p$  index. When  $k_p$  is low (below about 4), the magnetosphere is quiet; when  $k_p$  is high, the magnetosphere is stormy. As Fig. 5 shows, it was

stormy on 14 November but quiet on 15 and 16 November 1998. The midpanel plots the electron flux measured by the GOES satellite. The flux fluctuates wildly during stormy periods. The ambient ion spectrum (not shown) measured on DSCS also did not show stormy or unusual behavior on 16 November. It is well known that during severe geomagnetic storms or substorms, spacecraft charging sometimes occurs if the ambient plasma becomes energetic. There was no charging on the DSCS satellite on 14 and 15 November, although two brief instantaneous events (about 3000 and 10,000 s universal time) were recorded on 16 November (top panel). Because 16 November 1988 was a quiet day (not stormy), any cause of charging due to hot ambient plasma is ruled out. The peak of the Leonids shower of 1998 arrived on 16 November 1998 but not at the time of the two charging events. It is tempting to associate the charging events with meteor impacts, but the true cause is unknown.

A basic theorem in spacecraft charging states that in a Maxwellian plasma environment, there exists a critical, or threshold, plasma electron temperature for surface charging to occur.<sup>2,19</sup> The reason for this theorem is as follows. At equilibrium, Kirchhoff's circuit law requires the surface potential  $\phi$  be determined by a current balance equation. In space and in the laboratory, the electron current is normally two orders<sup>42,43</sup> of magnitude greater than that of ions because ions are much heavier and slower. Because an initially uncharged spacecraft placed in a plasma would intercept more electrons than ions because of mass difference, the spacecraft would charge to a negative potential, which renders the fluxes to balance at equilibrium.

Photoelectrons are important in sunlight. Low-level positive charging occurs when the ambient plasma environment is quiet while the surface is in sunlight.<sup>1</sup> The level is low because the dominant sunlight spectral line, Lyman- $\alpha$ , has about 10.2 eV, whereas the work function of most surface materials is about 4–5 eV, resulting in photoelectron energies of a few electron volts only. When the charging level exceeds a few electron volts, the photoelectrons can not leave. Thus, low-level charging by sunlight, at geosynchronous orbits, for example, is up to a few electron volts only. However, if the spacecraft is near the sun, the far UV lines become more intense. As a result, more high-energy (tens of electron volts) photoelectrons will come out, in contrast to the geosynchronous orbit case where the photoelectrons are of 1 to few electron volts only. Consequently, the spacecraft can charge to tens- of volts (positive) when approaching the sun, in contrast to 1 or few volts at the geosynchronous orbits.

We consider negative charging here because, for the case under discussion, the spacecraft interacts with the plasma generated by meteoroid impact. Charging by plasmas needs to be explained clearly. Electron flux is higher than ion flux because of mass difference. Therefore, any uncharged object placed in a plasma would

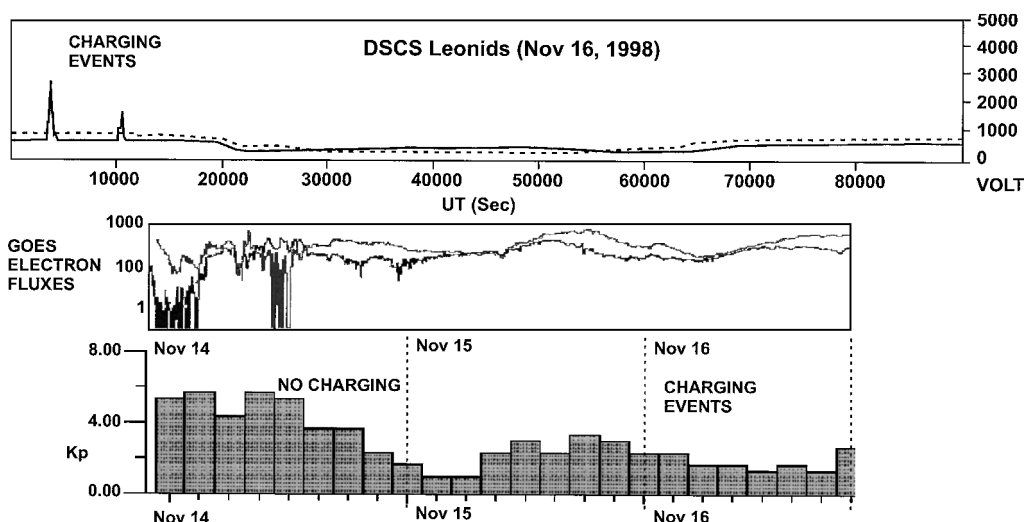


Fig. 5 Top: Two brief charging events of kV magnitude (negative voltage) on the DSCS satellite, 16 Nov. 1998; none was on 14 and 15 Nov. Middle: GOES satellite measurements showing moderately stormy plasma condition on 14 Nov. but quiet condition on 16 Nov. Bottom: geomagnetic index showing low  $k_p$  on 16 Nov. (The GOES and  $k_p$  data were obtained from the Space Environment Center, Boulder, CO, National Oceanic and Atmospheric Administration, U.S. Department of Commerce.)

intercept more electrons than ions. As a result, the object becomes negatively charged to an equilibrium potential, which renders the incoming flux of electrons to equal the ion flux. The rendering is carried out by the repulsion (to electrons) and the attraction (to ions) of the negative potential.

To calculate the onset of negative charging, it is often a good approximation to ignore the ions because the ion flux is orders of magnitude smaller than the electron flux. The approximate current balance is, therefore, between the incoming ambient electrons and the outgoing secondary and backscattered electrons:

$$\int_0^\infty dE E f(E) = \int_0^\infty dE E f(E) [\delta(E) + \eta(E)] \quad (10)$$

In Eq. (10), the left-hand side represents the incoming electron flux with an energy distribution  $f(E)$ ; the right-hand side represents that of the outgoing electrons. Here,  $\delta(E)$  and  $\eta(E)$  are the secondary and backscattered electron coefficients. It is more convenient to use energy integration than velocity integration because the coefficients are measured as functions of energy. For normal electron incidence, the angular variables cancel in Eq. (10). For angle-distributed incoming flux, the coefficients have to be angle dependent and the angular integrations have to be included.<sup>19</sup>

Substituting the Maxwellian distribution  $f(E)$ ,

$$f(E) = n(m_e/2\pi kT)^{1/2} \exp(-E/kT) \quad (11)$$

in the current balance equation (10), one finds that the density  $n$  cancels on both sides. Thus, if the assumption is made that the energy distribution of the impact generated plasma is Maxwellian, the current balance [Eq. (10)] is independent of the plasma density  $n$  and is a function of electron temperature  $T$  only. This is an important theorem. The solution  $T^*$  of Eq. (10) is the critical, or threshold, temperature for the onset of surface charging. Typical values of  $T^*$  are 1000–2000 eV depending on the surface material.<sup>2,19,43</sup> For  $\text{SiO}_2$ , for example,  $T^*$  is 1.7 keV for normal electron incidence and 2.6 keV for isotropic incidence. Thus, if the plasma electron temperature is below 1.7 keV, a silicon dioxide surface charging onset cannot occur.

When 70-nm boron carbide projectiles of 94 km/s were used on aluminum surfaces in the laboratory, it was found that 2.9% of the projectile energy went to the plasma kinetic energy, 0.5% went to ionizing the neutrals to form plasma, and 0.3% went to vaporizing the neutrals.<sup>14</sup> The hydrogen line in the plasma showed 120 eV and the carbon line 40 eV. Grün (personal communication, 2000) also observed that the impact of meteor-sized projectile generated plasma energy of typically 10 to a few tens of electron volts only. In any case,

the energy distribution of the impact-generated plasma has not been measured. If the assumption is made that the energy distribution of the impact-generated plasma is Maxwellian, the plasma temperature is the key factor determining whether significant negative-voltage charging can occur. Because the impact-generated plasma has an approximate mean energy of 10–120 eV only, the plasma electron temperature is well below the critical temperature  $T^*$  for negative charging to occur. Thus, no negative charging onset would occur for the spacecraft interacting with the plasma generated by meteor impact. Because the spacecraft charging theorem is independent of the plasma density  $n$ , the preceding result is independent of how much plasma is generated on meteor impact.

### Sudden and Net Charge Emission

If the charge produced on neutral particle impact is not neutral, meaning there is a net charge of one sign produced from the impact site and its neighborhood (Fig. 6), charging would result. Earlier measurements of separate charge production have been reviewed by Pailer and Grün.<sup>44</sup> The authors concluded<sup>44</sup> that a typical value for electron yield  $Y_e$  due to neutral particle impact is 0.2–0.4, relatively independent of the particle energy, provided that the latter exceeds the ionization threshold. The electron (or ion) yield is the number of impact-generated electrons (or ions) emitted from or near the impact site per impacting particle. Their ion yield<sup>44</sup> seems inconclusive, varying widely from 0.01 to 2. Later measurements<sup>45,46</sup> confirmed the value 0.2 for  $Y_e$  and reported 0.04 for  $Y_i$ , the yield of ions. Schmidt and Arends<sup>46</sup> used aluminum, gold, and white paint as targets and Xe, Ar, Kr, and air molecules as beam species, whereas Rudenauer and Steiger<sup>45</sup> used Xe and Ar as neutral particle beams and an aluminum alloy as target. Whereas these results are indicative of higher electron yield than that of ions, the energies of the electrons and ions have not been measured. The yields and energies are important for determining the level of charging, as discussed in the next paragraph.

Even a small imbalance of electron and ion yields would produce a substantial net charge on impact by a meteoroid, if the yields are large. The spacecraft potential is determined by current balance. At geosynchronous altitudes, the ambient current is of the order of milliamperes.<sup>19,25</sup> For an emitted electron current exceeding the ambient currents, the former controls the current balance, driving the spacecraft positive in voltage. If, however, the emitted electrons have a few electron volts only, the charging level cannot exceed a few volts.

Our conjecture is that the higher electron yield ( $Y_e > Y_i$ ) is due to the secondary electrons coming out from beneath the surface of the target material in the neighborhood of the impact crater. Secondary

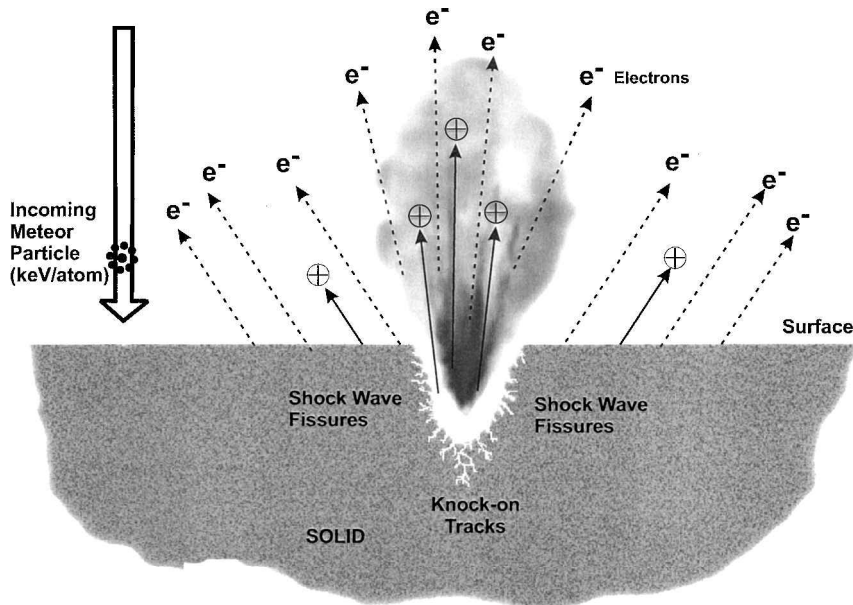


Fig. 6 Plasma and neutral gas generated by the hypervelocity impact of a particle on a solid surface.

electrons have typically a few electron volts in energy. Charging cannot exceed a few volts if the emitted electrons have only a few electron volts.

### Triggering Spacecraft Discharges

As discussed already, hypervelocity particulate impact on spacecraft may produce 1) mechanical damage to the spacecraft and 2) plasma and neutral vapor that pose a hazard to electrical systems. These effects are not mutually exclusive and may occur at the same time; next is a brief presentation of scenarios where these hazards can play a role.

A potential weak point susceptible to hypervelocity impact hazards are the exposed cables on a spacecraft (scenario 1). The cable sheath may have weathered as a result of years of operation in the harsh space environment. Depending on the energy of the impacting particle and the strength of the target material, the impacting particle may penetrate or even tear apart the worn cable sheath and cause electrical disruption to the circuits. A case in point is the failure of MSTI-2 satellite, which was attributed to the impact of orbital debris on a wire bundle.<sup>18,47</sup>

Another potential weak point pertaining to this type of problem is the solar panel power system,<sup>48</sup> as illustrated in Fig. 7 (scenario 2). We have shown that, over the course of a satellite lifetime, the probability for meteor impacts of solar panels to depths of 5 mm is quite high. Such a depth is sufficient to cause great damage to the solar panels. A large Leonids meteoroid, though rare, may penetrate deeper. A case in point is the failure of the Olympus satellite. It occurred suddenly during the time of maximum activity of a Perseids shower. The time was in a geomagnetically quiet period, which rules out surface and deep dielectric charging as a cause. The gyro and its power supply failed. The cause was attributed to a meteoroid hit on the solar panel system or a cable connecting the system to the gyro.<sup>18,47,49</sup>

If the impact occurs near solar cells that are at different potentials, the impact-generated plasma might then connect the different solar cells (scenario 3). The number of electrons is maintained constant or increases in time, provided that the number of electrons  $m$  generated between a cathode and an anode sustains or increases in time. This process is not limited to solar cells (Fig. 7) but is applicable to two or more nearby differentially charged configurations. We discuss now two scenarios in which the number of electrons is maintained constant or increases in time.

Let  $\mu$  ionization events be generated in the neutral gas by an electron transit between a cathode and an anode. Both the electrons and the neutral gas are produced by a meteor impact on a surface. The cathode and anode can be two nearby differentially charged surfaces. The  $\mu$  electrons are accelerated toward the anode, and the  $\mu$  ions are accelerated toward the cathode. If an ion impact on the cathode can produce  $\gamma$  electrons, then  $\mu$  ion impacts would produce  $\mu\gamma$  electrons from the cathode. A necessary condition to sustain the discharge is the inequality

$$\mu\gamma \geq 1 \quad (12)$$

The newly created electron would start its journey toward the anode, thereby creating at least  $\mu$  new electron-ion pairs to sustain a low-level discharge or initiate an avalanche ionization.

We now calculate the quantity  $\mu$ . Let  $\alpha$  ionizations be generated by an electron traveling through a distance  $dx$ . For  $n$  electrons at  $x$ , the number of ionizations at  $x + dx$  is given by

$$dn = n\alpha dx \quad (13)$$

The total number of ionizations from the cathode ( $x = 0$ ) to an anode ( $x = d$ ) is given by

$$n(d) = n(0) \exp(\alpha d) \quad (14)$$

where  $n(0)$  is the initial number of electrons starting the journey at  $x = 0$ . Thus,  $\mu = \exp(\alpha d)$ .

For electron impact ionization of neutral gas,  $\alpha$  is given by<sup>50</sup>

$$\alpha \propto N \int dE E^{\frac{1}{2}} f(E) \sigma(E) \quad (15)$$

where  $N$  is neutral density and  $E$  the electron energy. Thus,

$$\mu = \exp \left[ Nd \int dE E^{\frac{1}{2}} f(E) \sigma(E) \right] \quad (16)$$

Applying the result [Eq. (16)] to discharges in meteor-generated plasma, we see that  $\mu$  is proportional to  $\exp(N)$  and depends on the integral of the electron density distribution function  $f(E)$ . Thus, both the neutral gas density and the plasma electron distribution function play important roles in mediating a discharge. The effect of a sustained low-level discharge can drain currents and degrade systems. An avalanche discharge can short a circuit or cause power supply failure rapidly.

We have shown the roles of two key players, namely, the plasma and the neutral vapor, both generated by meteor impacts on surfaces. The inequality [Eq. (12)] is necessary but not sufficient. To be sufficient, one needs to account for loss mechanisms, a situation reminiscent of the discharge criteria in critical ionization velocity.<sup>51</sup>

A heretofore unsuspected differentially charged configuration is dielectric surface materials impregnated with incoming high-energy (megaelectron volts or higher) electrons and ions (scenario 4). During a passage of a high-energy (megaelectron volts or higher) plasma cloud or a solar coronal mass ejection (CME) cloud, the energetic (megaelectron volts or higher) electrons and ions penetrate into materials to different depths and stay there, if the conductivity is low. For example, megaelectron volt electrons penetrate to  $10^2$  mil in aluminum, whereas megaelectron volt protons to  $4 \times 10^{-1}$  mil only.<sup>2</sup> After many hours or days, a double layer is formed inside the dielectric. The electron flux in space is two orders of magnitude greater than that of ions.<sup>42,43</sup> However, with a predominantly electron layer formed inside, the dielectric surface and its vicinity experience an electric field that attracts ions. When the ambient environment becomes quiet after days of energetic cloud passage, the ambient plasma returns to low energy again. Low-energy ions can be attracted by the surface electric field, thus building up the shallow ion layer. Nature tends to evolve toward neutralization and equilibrium. Even if the low-energy ions can completely neutralize the surface electric field, they cannot recombine with the deeply layered electrons because they are separated at a distance. Thus, a nonequilibrium configuration ensues and is unstable. Shorting the two layers would lead to a discharge, which is called an anodized discharge.<sup>52</sup> A hypervelocity meteor impact penetration can trigger such shorting (Fig. 8) because the ionization track made by the meteor impact can provide a conduction channel for a discharge between the electrons and ions staying at different depths. A case in point is the recent failures of three geosynchronous communication satellites, namely, ANIK-1, AT&T Telstar-401, and Motorola Galaxy-4. Although the true causes of their failures may never be known, all three of them occurred after (but not during) the passage of a CME.

Another hazardous scenario combining the penetration and plasma/vapor production properties of hypervelocity particulate impact is as follows (scenario 5). Depending on the momentum of the meteoroid or particulate and the thickness/strength of the wall, complete penetration may occur. If the penetration goes through a wall,

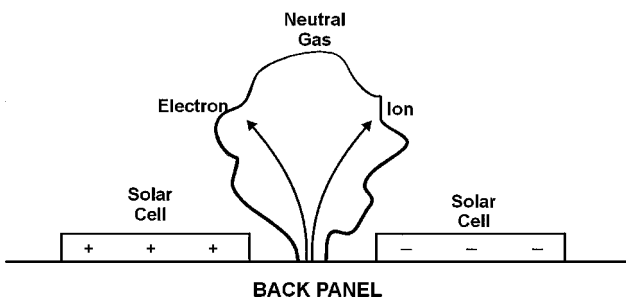


Fig. 7 Electrons, ions, and neutral gas generated by a hypervelocity impact on a solar panel.

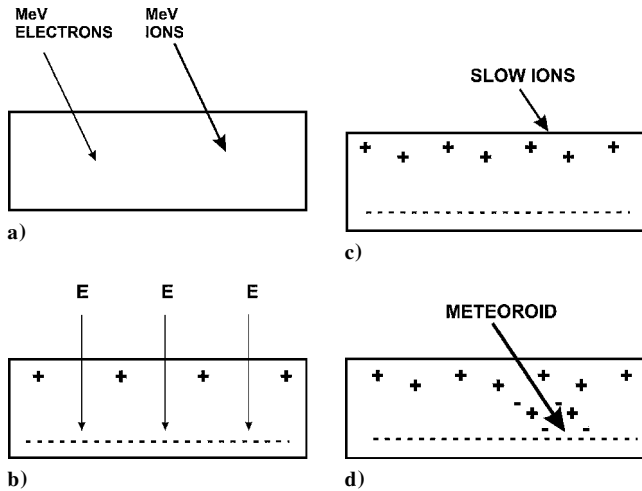


Fig. 8 Sequence (a, b, c, d) of double-layer formation in a dielectric material.

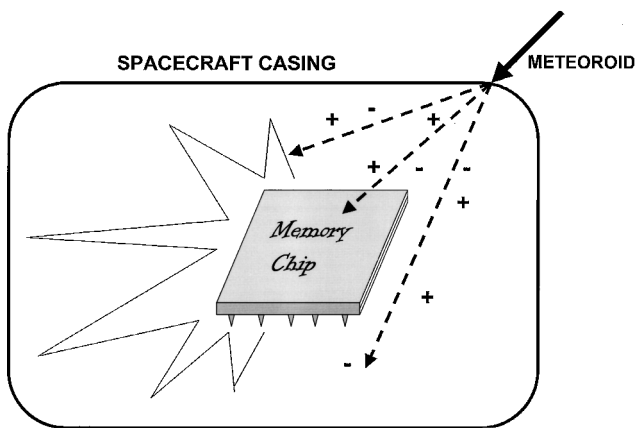


Fig. 9 Meteoroid penetrating through the spacecraft casing.

the plasma and neutral vapor can come out from the other side of the wall. This would have important consequence for the electronics inside. The exposed wires inside and the circuit boards may be shorted. The alkali vapor released from the meteoroid may react chemically with certain materials such as aluminum (Fig. 9). For example, sodium, which is known to be reactive, can react with aluminum-bearing minerals to produce the sodium aluminosilicate<sup>53</sup>  $\text{NaAlSi}_3\text{O}_8$ .

The generation of plasma by a sudden impact can produce electromagnetic waves,<sup>54</sup> which then can introduce noise and spurious signals into the antenna system<sup>55–58</sup> (scenario 6). Finally, we briefly point out that, as an impact occurs, the rapid burst of neutral gas, electrons, and ions would give off a flash of optical and electromagnetic radiation signatures. The optical lines of the flash would depend on the compositions of the spacecraft surface and the meteoroid or debris. Collisions, excitation, ionization, and recombination occur in a short period before diffusion transport takes over. The optical emission and even the impact-generated dust cloud itself can temporarily degrade the performance of optical instruments onboard. Dust attachment or molecular adsorption on optical instruments could be hazardous. A more detailed discussion of this subject is beyond the scope of this paper.

### Mitigation

Meteors are rarely taken into consideration when designing spacecraft. It is simply assumed that the risk is low. There are, however, a few mitigation methods that have been employed in the past. The most common methods for reducing the impact of meteoroids on spacecraft are preventive in nature. These methods consist of 1) minimization of the probability of meteoroid impacts, 2) minimization of the risk of a short circuit or a discharge should an impact occur, and 3) protection of sensitive electronics behind some shields to avoid impact penetration.

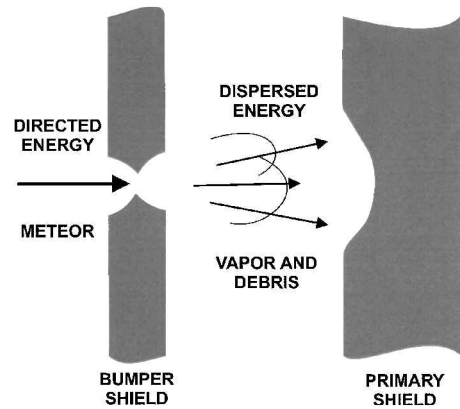


Fig. 10 Whipple shield.

In anticipation of an intense meteor shower, it is possible to orient the solar panels in a direction parallel to the meteor stream. This minimizes the effective area normal to the meteor stream velocity so that the probability of a strike is minimized. It is also possible to turn sensitive instruments, such as optics, away from the direction in which shower meteors will come. Another common practice is to shut off all of the nonessential electrical power on a spacecraft, during the period of an intense meteor shower, to minimize the probability of a short circuit or a discharge in case an impact occurs. Moving a spacecraft to the side of the Earth opposite the shower radiant, thereby using the Earth as a shield, would also be helpful, but moving a spacecraft is often a difficult task.

Whipple<sup>59</sup> suggested a double-wall shield, comprising a bumper shield and a primary shield. If an impinging particle penetrates through the bumper shield, the molten particle or vapor generated, together with the small debris from the bumper, will impact the primary shield with dispersed instead of direct energy (Fig. 10). This provides a better opportunity for shielding. Modern designs of multiwall systems using high-strength composite materials are improvements over the original Whipple design (see Ref. 60). Note, however, that few satellite employ the Whipple shield.

### Conclusions

We have emphasized the hazards of hypervelocity particle impacts in space. Hypervelocity particles generate great energies on impact on spacecraft surfaces. Based on other laboratory measurements of impact penetration depth, empirical formulas of penetration, and plasma production, we have pointed out the importance of charge imbalance in the plasma produced on impact. As shown in the discussion, charge imbalance can cause spacecraft charging. We have also discussed some worst-case scenarios that may arise from hypervelocity impact on spacecraft. To sustain a diode-type discharge, it is necessary to satisfy a simple Townsend-type inequality. The sufficient conditions would require accounts of loss mechanisms. An optical or electromagnetic flash, with characteristic signature lines, may result from hypervelocity impact.

### References

- <sup>1</sup>Lai, S. T., Aggson, T., McNeil, W. J., and Cohen, H. C., "Boom Potential on a Rotating Satellite in Sunlight," *Journal of Geophysical Research*, Vol. 91, No. A11, 1986, pp. 12,137–12,141.
- <sup>2</sup>Hastings, D. E., and Garrett, H. B., *Spacecraft-Environment Interactions*, Cambridge Univ. Press, Cambridge, England, U.K., 1996, pp. 142–206.
- <sup>3</sup>Vampola, A. L., "Thick Dielectric Charging on High-Altitude Spacecraft," *Journal of Electrostatics*, Vol. 20, 1987, pp. 21–30.
- <sup>4</sup>Reinhard, R., "The Giotto Spacecraft Impact-Induced Plasma Environment," edited by R. Reinhard, ESA-SP-224, ESA, Paris, 1984, pp. 1–104.
- <sup>5</sup>Beech, M., and Brown, P., "Space-Platform Impact Probabilities—The Threat of the Leonids," *ESA Journal*, Vol. 18, No. 1, 1994, pp. 63–72.
- <sup>6</sup>Beech, M., Brown, P., and Jones, J., "The Potential Danger to Space Platform from Meteor Storm Activity," *Quarterly Journal of the Royal Astronomical Society*, Vol. 36, No. 2, 1995, pp. 127–152.
- <sup>7</sup>Beech, M., Brown, P., Jones, J., and Webster, A. R., "The Danger to Satellites from Meteor Storms," *Advances in Space Research*, Vol. 20, No. 8, 1997, pp. 1509–1512.



- <sup>8</sup>Foschini, L., and Cevolani, G., "Impact Probabilities of Meteoroid Streams with Artificial Satellites: An Assessment," *Il Nuovo Cimento*, Vol. 20C, No. 2, 1997, pp. 211-215.
- <sup>9</sup>Grün, E., and Staubach, P., *Physics, Chemistry, and Dynamics of Interplanetary Dust*, edited by B. Å. S. Gustafson and M. S. Hanner, Vol. 104, Astronomical Society of the Pacific, San Francisco, 1996, pp. 3-14.
- <sup>10</sup>Mandeville, J. C., "Study of Cosmic Dust Particles on Board LDEF: The FRECOA Experiment," *Advances in Space Research*, Vol. 11, No. 12, 1991, pp. 101-107.
- <sup>11</sup>McDonnell, J. A. M., and Sullivan, K., "Hypervelocity Impacts on Space Detectors: Decoding the Projectile Parameters," *Proceeding of the Workshop on Hypervelocity Impacts in Space*, Univ. of Kent, Canterbury, England, U.K., 1991.
- <sup>12</sup>Krueger, F. R., "Ion Formation by High- and Medium Velocities Dust Impacts from Laboratory Measurements and Halley Results," *Advances in Space Research*, Vol. 17, No. 12, 1996, pp. 71-75.
- <sup>13</sup>McDonnell, J. A. M., McBride, N., and Gardner, D. J., "The Leonid Meteoroid Stream: Spacecraft Interactions and Effects," *Second European Conference on Space Debris*, European Space Operations Centre, Darmstadt, Germany, 1997, pp. 391-396.
- <sup>14</sup>Ratcliff, P. R., and Allahdadi, F., "Characteristics of the Plasma from a 94 kms<sup>-1</sup> Microparticle Impact," *Advances in Space Research*, Vol. 17, No. 12, 1996, pp. 87-91.
- <sup>15</sup>Gleghorn, G. (Chair, Committee on Space Debris), *Orbital Debris—A Technical Assessment*, National Academy Press, Washington, DC, 1995, pp. 1-9.
- <sup>16</sup>Flury, W., "Collision Probability and Spacecraft Disposition in the Geostationary Orbit," *Advances in Space Research*, Vol. 11, No. 12, 1991, pp. 67-79.
- <sup>17</sup>Rossi, A., Anselmo, L., Cordelli, A., Farinella, P., and Pardini, C., "Modelling the Evolution of the Space Debris Population," *Planetary and Space Science*, Vol. 46, No. 11/12, 1998, pp. 1583-1596.
- <sup>18</sup>Koons, H. C., Mazur, J. E., Selesnick, R. S., Blake, J. B., Fennell, J. F., Roeder, J. L., and Anderson P. C., "The Impact of the Space Environment on Space Systems," Rept. TR-99(1670)-1, The Aerospace Corp., El Segundo, CA, 1999, pp. 91, 116, 117, 131, 141, 144, 147, 149.
- <sup>19</sup>Lai, S. T., "Spacecraft Charging Thresholds in Single and Double Maxwellian Space Environments," *IEEE Transactions on Nuclear Science*, Vol. 119, No. 6, 1991, pp. 1629-1634.
- <sup>20</sup>Lai, S. T., "Mott Transition as a Cause of Anomalies on Spacecraft," *IEEE Transactions on Plasma Science*, Vol. 28, No. 6, 2000, pp. 2097-2102.
- <sup>21</sup>Taylor, A. D., Baggaley, W. J., and Steel, D. I., "Discovery of Interstellar Dust Entering the Earth's Atmosphere," *Nature*, Vol. 380, No. 6521, 1996, pp. 323-325.
- <sup>22</sup>Hawkes, R. L., Close, T., and Woodsworth, S., "Meteoroids from Outside the Solar System," *Meteoroids 1998*, edited by W. J. Baggaley and V. Porubcan, Astronomical Inst., Slovak Academy of Science, Bratislava, Slovakia, 1999, pp. 257-264.
- <sup>23</sup>Cepelcha, Z., Borovicka, J., Elford, W. G., Revelle, D. O., Hawkes, R. L., Porubcan, V., and Simek, M., "Meteor Phenomena and Bodies," *Space Science Review*, Vol. 84, No. 3/4, 1998, pp. 327-471.
- <sup>24</sup>Foschini, L., "The Meteoroid Hazard for Space Navigation," *Secondo Convegno Nazionale di Scienze Planetarie*, Alenia Aerospazio, Turin, Italy, 1998, pp. 131-143.
- <sup>25</sup>Cevolani, G., and Foschini, L., "The Effects of Meteoroid Stream Enhanced Activity on Human Space Flight: An Overview," *Planetary Space Science*, Vol. 46, No. 11/12, 1998, pp. 1597-1604.
- <sup>26</sup>Cour-Palais, B. G., "Hypervelocity Impact in Metals, Glass, and Composites," *International Journal of Impact Engineering*, Vol. 5, No. 1-4, 1987, pp. 221-237.
- <sup>27</sup>Tribble, A. C., *The Space Environment*, Princeton Univ. Press, Princeton, NJ, 1995, p. 171.
- <sup>28</sup>Fisher, A. A., Hawkes, R. L., Murray, I. S., Campbell, M. D., and LeBlanc, A. G., "Are Most Meteoroids Really Dustballs?," *Planetary Space Science*, Vol. 48, No. 10, 2000, pp. 911-920.
- <sup>29</sup>Öpik, E. J., *Physics of Meteor Flight in the Atmosphere*, Interscience, New York, 1958, p. 148.
- <sup>30</sup>McNeil, W. J., Dressler, R. A., and Murad, E., "Impact of a Major Meteor Storm on Earth's Ionosphere: A Modeling Study," *Journal of Geophysical Research*, Vol. 106, No. A6, 2001, pp. 10,447-10,466.
- <sup>31</sup>Sarma, T., and Jones, J., "Double-Station Observations of 454 TV Meteors. I. Trajectories," *Bulletin of the Astronomical Institutes of Czechoslovakia*, Vol. 36, No. 1, 1985, pp. 9-24.
- <sup>32</sup>Sarma, T., and Jones, J., "Double-Station Observations of 454 TV Meteors. II. Orbits," *Bulletin of the Astronomical Institutes of Czechoslovakia*, Vol. 36, No. 2, 1985, pp. 103-115.
- <sup>33</sup>Brown, P., Campbell, M. D., Ellis, K. J., Hawkes, R. L., Jones, J., Gural, P., Babcock, D. D., Barnbaum, C., Barlett, R. K., Medard, M., Bedient, J., Beech, M., Brosch, N., Clifton, S., Connors, M., Cooke, B., Goetz, P., Gaines, J. K., Gramer, L., Gray, J., Hildebrand, A. R., Jewell, D., Jones, A., Leake, M., LeBlanc, A. G., Looper, K. K., McIntosh, B. A., Montague, T., Morrow, M. J., Murray, I. S., Nikolova, S., Robichaud, J., Sponder, R., Talarico, J., Theijsmeijer, C., Tilton, B., Treu, M., Vachon, C., Webster, A. R., Weryk, R., and Worden, S. P., "Global Ground-Based Electro-Optical and Radar Observations of the 1999 Leonid Shower: First Results," *Earth Moon Planets*, Vol. 82-83, No. 1-3, 2000, pp. 167-190.
- <sup>34</sup>Campbell, M. D., Brown, P. G., LeBlanc, A. G., Hawkes, R. L., Jones, J., Worden, S. P., and Correll, R. R., "Electro-Optical Results from the 1998 Leonid Shower: I. Atmospheric Trajectories and Physical Structure," *Meteorites and Planetary Science*, Vol. 35, No. 6, 2000, pp. 1259-1268.
- <sup>35</sup>Pawlowski, J., "Johnson Space Center's Leonid Optical Observations," *Meteorites and Planetary Science*, Vol. 34, No. 6, 1999, pp. 945-947.
- <sup>36</sup>Pawlowski, J., and Hebert, T., "The Leonid Meteors and Space Shuttle Risk Assessment," *Earth Moon Planets*, Vol. 82-83, No. 1-3, 2000, pp. 149-190.
- <sup>37</sup>Jenniskens, P., "Meteor Stream Activity I. The Annual Streams," *Astronomy and Astrophysics*, Vol. 287, No. 7, 1994, pp. 990-1013.
- <sup>38</sup>Hughes, D. W., "Meteors," *Cosmic Dust*, edited by J. A. M. McDonnell, Wiley, Chichester, England, U.K., 1978, pp. 123-186.
- <sup>39</sup>Brown, P., and Arlt, R., "Final Results of the 1996 Leonid Maximum," *WGN, Journal of the IMO*, Vol. 25, No. 5, 1997, pp. 210-214.
- <sup>40</sup>Purvis, C., Garrett, H. B., Whittlesey, A. C., and Stevens, N. J., "Design Guidelines for Assessing and Controlling Spacecraft Charging Effects," NASA TP 2361, 1984.
- <sup>41</sup>Lai, S. T., "An Improved Langmuir Probe Formula for Modeling Satellite Interactions with Near Geostationary Environment," *Journal of Geophysical Research*, Vol. 99, No. A1, 1994, pp. 459-468.
- <sup>42</sup>Reagan, J. B., Meyerott, R. E., Nightingale, R. W., Filbert, P. C., and Imhoff, W. L., "Spacecraft Charging Currents and Their Effects on Space Systems," *IEEE Transactions on Electrical Insulation*, Vol. 18, No. 3, 1983, pp. 354-365.
- <sup>43</sup>Lai, S. T., and Della-Rose, D. J., "Spacecraft Charging at Geosynchronous Altitudes: New Evidence of Existence of Critical Temperature," *Journal of Spacecraft and Rockets*, Vol. 38, No. 6, 2001, pp. 922-928.
- <sup>44</sup>Pailer, N., and Grün, E., "Production of Secondary Particles by Neutral and Ionized Cometary Gas and Dust Impacting on the Shield of the Giotto Spacecraft," SP 187, ESA, 1982, pp. 1-14.
- <sup>45</sup>Rudener, F. G., and Steiger, W., "Measurements of Secondary Charged Particle Emission Under Ion Neutral Impact," SP 224, ESA, 1984, pp. 1-10.
- <sup>46</sup>Schmidt, R., and Arends, H., "Measurements of Integral Yields of Charged Secondary Particles Using Neutral Beams Simulating a Cometary Fly-by," SP 224, ESA, 1984, pp. 15-20.
- <sup>47</sup>Herr, J. L., "Review and Comments on MSTI-2 Failure Report," Rept. 212-010-94-017, NASA Marshall Space Flight Center, Dec. 1994.
- <sup>48</sup>Berthoud, L., and Paul, K., "Meteoroid and Debris Micro-Impacts on Space-Exposed Solar Arrays," *Advances in Space Research*, Vol. 20, No. 8, 1997, pp. 1441-1445.
- <sup>49</sup>Caswell, R. D., McBride, N., and Taylor, A., "Olympus End of Life Anomaly—A Perseid Meteor Impact Event?," *International Journal of Impact Engineering*, Vol. 17, No. 1-3, 1995, pp. 139-146.
- <sup>50</sup>von Engel, A., *Electric Plasmas: Their Nature and Uses*, Interscience, New York, 1983, p. 129.
- <sup>51</sup>Lai, S. T., and Murad, E., "Inequality Conditions for Critical Velocity Ionization Space Experiments," *IEEE Transactions on Plasma Science*, Vol. 20, No. 6, 1992, pp. 770-777.
- <sup>52</sup>Lai, S. T., "Some Space Hazards of Spacecraft Surface and Bulk Charging," *Proceedings of the 7th Spacecraft Charging Technology Conference* (to be published).
- <sup>53</sup>Lewis, J. S., *Physics and Chemistry of the Solar System*, Academic Press, London, 1995, p. 95.
- <sup>54</sup>Foschini, L., "On the Interaction of Radio Waves with Meteoric Plasma," *Astronomy and Astrophysics*, Vol. 341, 1999, pp. 634-639.
- <sup>55</sup>Foschini, L., "Electromagnetic Interferences from Plasmas Generated in Meteoroid Impacts," *Europhysics Letters*, Vol. 43, No. 2, 1998, pp. 226-229.
- <sup>56</sup>Meyer-Vernet, N., and Perche, C., "Plasma Tool Kit for Antennae and Thermal Noise Near the Plasma Frequency," *Journal of Geophysical Research*, Vol. 94, No. A3, 1989, pp. 2405-2415.
- <sup>57</sup>Meyer-Vernet, N., Couturier, P., Hoang, S., Perche, C., Steinberg, J. L., Fainberg, J., and Meete, C., "Plasma Diagnosis from Thermal Noise and Limits on Dust Flux or Mass in Comet Giacobini-Zinner," *Science*, Vol. 232, April 1986, pp. 370-374.
- <sup>58</sup>Meyer-Vernet, N. P., "Quasi-Thermal Noise Corrections due to Particle Impacts or Emission," *Journal of Geophysical Research*, Vol. 88, No. A10, 1983, pp. 8081-8093.
- <sup>59</sup>Whipple, F. L., "Meteorites and Space Travel," *Astronomical Journal*, Vol. 131, 1947, p. 1161.
- <sup>60</sup>Schonberg, W. P., "Protecting Spacecraft Against Orbital Debris Impact Damage Using Composite Materials," *Symposium on Recent Developments in the Study of Impacts on Composite Materials*, Virginia Polytechnic Inst. and State Univ., Blacksburg, VA, 1999.